



MambaCSR: Dual-Interleaved Scanning for Compressed Image Super-Resolution With SSMs

Yulin Ren¹, Xin Li^{1✉}, Mengxi Guo², Bingchen Li¹, Shijie Zhao² and Zhibo Chen^{1✉}

¹University of Science and Technology of China, ²Bytedance Inc.

{renyulin, lbc31415926}@mail.ustc.edu.cn,

{xin.li, chenzhibo}@ustc.edu.cn, {guomengxi.qoelab, zhaoshijie.0526}@bytedance.com

Abstract

We present MambaCSR, a simple but effective framework based on Mamba for the challenging compressed image super-resolution (CSR) task. Particularly, the scanning strategies of Mamba are crucial for effective contextual knowledge modeling in the restoration process despite it relying on selective state space modeling for all tokens. In this work, we propose an efficient dual-interleaved scanning paradigm (DIS) for CSR, which is composed of two scanning strategies: (i) hierarchical interleaved scanning is designed to comprehensively capture and utilize the most potential contextual information within an image by simultaneously taking advantage of the local window-based and sequential scanning methods; (ii) horizontal-to-vertical interleaved scanning is proposed to reduce the computational cost by leaving the redundancy between the scanning of different directions. To overcome the non-uniform compression artifacts, we also propose position-aligned cross-scale scanning to model multi-scale contextual information. Experimental results on multiple benchmarks have shown the great performance of our MambaCSR in the compressed image super-resolution task. The code will be soon available in <https://github.com/renyulin-f/MambaCSR>.

1 Introduction

Compressed Image Super-Resolution (CSR) has gradually emerged as an advanced task in industrial applications and human life, intending to remove the severe hybrid distortions caused by compression and low resolution simultaneously. In contrast to the existing single image super-resolution (SISR), CSR exhibits more non-uniform and diverse degradations including block artifacts, ringing effects, color drifting, etc., together with essential information loss. The above characteristics of CSR impose significant challenges for the contextual information modeling capability of existing super-resolution models.

A series of works have been explored to improve the contextual modeling capability through the framework design. The commonly used frameworks are usually based on three typical networks, including CNN [68, 29, 20], Transformer, and MLP. In particular, CNN excels at capturing local contextual information, while global contextual information must be aggregated by increasing the depth of networks. In contrast, Transformer-based works [8, 23] utilize the self-attention mechanism to build long-range contextual dependencies for tokens across images, which entails a large computational cost. Unlike the above works, MLP-like works [25] abandon the complex attention and successfully model the long-range contextual information with well-designed strategies for token mixers, significantly reducing the computational costs. Despite that, transformer-based works remain the mainstream for CSR tasks and deliver optimal performances. This raises a crucial question: "whether there exists a new framework that can outperform transformers in CSR tasks".

✉ Xin Li and Zhibo Chen are corresponding authors.

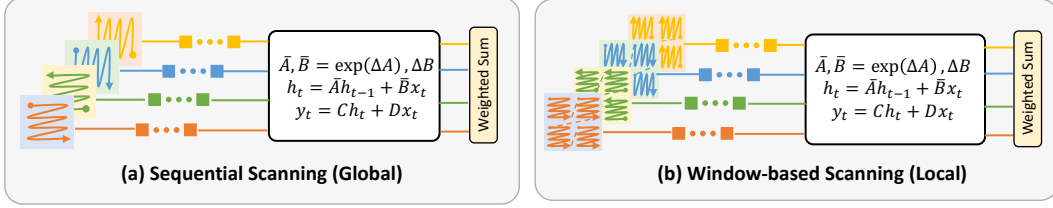


Figure 1: Comparisons of existing scanning methods. (a) Sequential scanning used in most low-level tasks [15, 42, 41]. (b) Local window-based scanning in some high-level tasks [19]

Fortunately, Mamba, a brand-new framework [12] is proposed in the NLP field, which takes advantage of the selective State Space Model (SSM) [13], thereby excelling at modeling long-range contextual information by dynamically deciding to preserve how much learned knowledge for each token in the scanning trajectory. Following this, lots of works have successfully applied the innovative framework to various visual fields, such as recognition [40], segmentation [47], and generation [44]. Thanks to the structure of SSM, the computational cost of Mamba is theoretically less than a transformer ($\mathcal{O}(n \log(n))$ versus $\mathcal{O}(n^2)$), which relieves the limitation of window-based representation learning in low-level vision with transformer. With the above advantages, some pioneering works have explored the Mamba framework for low-level vision tasks, *e.g.*, image restoration [15, 42], dehazing [71], and deraining [70]. However, the scanning strategies of the above works still follow early VMamba [30] and rely on two horizontal and vertical scanning trajectories as shown in Fig. 1 (a) for long-range dependencies modeling, which tends to neglect the exploration of local dependencies.

However, in the context of the CSR task, the diverse and uni-formed hybrid degradations pose the high requirements of excavating the most informative contextual information across the whole tokens within one image. Consequently, both the local dependencies and long-range contextual information are crucial for CSR tasks, which motivated us to investigate how to design one scanning strategy to achieve the most comprehensive contextual modeling in Mamba.

In this work, we present MambaCSR, the first Mamba-based framework for CSR, intending to activate the comprehensive contextual modeling capability of Mamba through our proposed dual-interleaved scanning (DIS) strategy. Typically, window-based scanning shown in Fig. 1(b) has been proven to be effective in capturing local dependencies for Mamba [19, 14]. Therefore, the hierarchical interleaved scanning of DIS is designed to iteratively apply window-based scanning and sequential-based scanning for MambaCSR, which aims to excavate both local and long-range contextual information simultaneously. From another perspective, the original VMamba exploits four types of scanning trajectories (*i.e.*, two horizontal and vertical scanning strategies) for contextual modeling. However, not all scanning trajectories are necessary/essential for each token in each operation, thereby being redundant. To reduce the computational cost, we propose to decouple four scanning trajectories and iteratively exploit two horizontal and vertical scanning trajectories in the adjacent layer, resulting in the horizontal-to-vertical interleaved scanning for DIS. With our proposed dual-interleaved scanning paradigm, MambaCSR exhibits excellent contextual modeling capability and efficiency for CSR tasks.

To further overcome non-uniformed degradations in CSR, we also introduce a position-aligned cross-scale scanning strategy for CSR, aiming at fusing the multi-scale contextual information, thereby increasing the non-uniformed representation capability. Notably, a naïve method is scanning the features of the down-sampled image and its corresponding original image. However, it ignores that most relevant contextual information across different scales is usually distributed in the same region. This motivates us to scan the tokens in the same position across scales first and move the scanning windows of both scales together. The above scanning strategy further improves the restoration capability of MambaCSR for complicated degradations in CSR. The main contributions of this paper are summarized as follows:

- We present MambaCSR, the first Mamba-based framework for CSR tasks, which introduces the dual-interleaved scanning (DIS) paradigm, intending to activate more comprehensive and efficient contextual information modeling for MambaCSR.

- To achieve the DIS paradigm, we propose (i) hierarchical interleaved scanning to fuse the local and long-range contextual information and (ii) horizontal-to-vertical scanning to reduce the computational redundancy for the contextual modeling of different tokens. Moreover, we propose the position-aligned cross-scale scanning strategy to fuse the multi-scale contextual information, thereby eliminating the non-uniformed degradations of CSR.
- Experimental results on various compressed benchmarks demonstrate the effectiveness and efficiency of our proposed MambaCSR.

2 Related Works

2.1 Compressed Image Super-resolution

Single image super-resolution (SISR) has been a long-standing research focus [6, 49, 62, 56, 24, 51, 37, 45, 48]. The pioneering work in this field is the CNN-based SRCNN [10]. Since then, numerous CNN-based models have emerged, incorporating deeper layers [20, 11, 29, 66], residual blocks [69], attention mechanisms [68, 9, 65], and non-local blocks [35, 53], significantly advancing SR performance. However, CNNs still struggle to capture long-range contextual information dependencies. Following the introduction of self-attention, Transformer-based SR models [4, 32, 64, 72, 61, 60] have been proposed, revolutionizing and dominating the SR field.

Based on this, compressed image super-resolution (CSR) has emerged as a new and crucial task closely tied to human life and industrial needs, originating from the AIM2022 competition [57]. This task focuses on processing downsampled, compressed low-resolution images, which present more severe artifacts than SISR, thereby imposing higher demands on model capabilities [22, 39]. The pioneering work in the CSR field is Swin2SR [8], based on the Swin-Transformer, which introduces several enhancements to SwinIR modules, improving training stability and better adapting to compressed distortions. Another notable example is HST [23], employing a hierarchical Swin Transformer to fuse multi-scale compressed information. CIBDNet [38] introduces a dual-branch framework that combines convolutional and transformer branches, further boosting performance. UCIP [25], based on an MLP framework integrated with prompt learning, achieves universal CSR tasks with high efficiency. Recently, the state space model has shown great potential in long-range modeling with linear complexity, making it a promising candidate for CSR tasks.

2.2 State Space Model in Vision Tasks

Recently, the State Space Model has demonstrated high efficiency in capturing the dynamics and dependencies of long sequences. This has garnered significant attention in the visual field, covering various domains including 3D visual recognition [67, 27], medical imaging [33, 54], multi-modal understanding [55, 58], remote sensing images [59, 16], and more. Due to its impressive potential performance gains, SSM has also been introduced into low-level vision tasks [15, 21, 73, 50]. Among these, MambaIR [15] employs 2D Selective Scanning (SS2D) [30] as the backbone while incorporating channel attention and convolutional layers to enhance local information capabilities. In contrast, VMambaIR [42], is based on a U-Net structure and extends channel dimension scanning for further feature extraction. FreqMamba [70] operates from the frequency domain, utilizing Mamba blocks to achieve improved de-raining effects. LFMamba [31] employs an efficient SS2D mechanism to achieve light-field image-super-resolution. However, most existing Mamba approaches [7] in the low-level field are preliminary explorations, relying primarily on the sequential scanning method. This approach overlooks the control over local information, which is critical in low-level tasks. In this paper, we introduce a dual-interleaved scanning method and a cross-scale scanning method to enhance the impact of local pixels and multi-scale features.

3 Approaches

In this section, we first review the basic theory of SSM in Sec.3.1. Then, we analyze the motivation of dual-interleaved scanning Sec.3.2 from the perspective of contextual modeling within SSM. Next, we provide a detailed explanation of the dual-interleaved scanning and cross-scale scanning methods in Sec.3.3 and Sec.3.4, respectively. Finally, we introduce the overall framework of MambaCSR in Sec. 3.5.

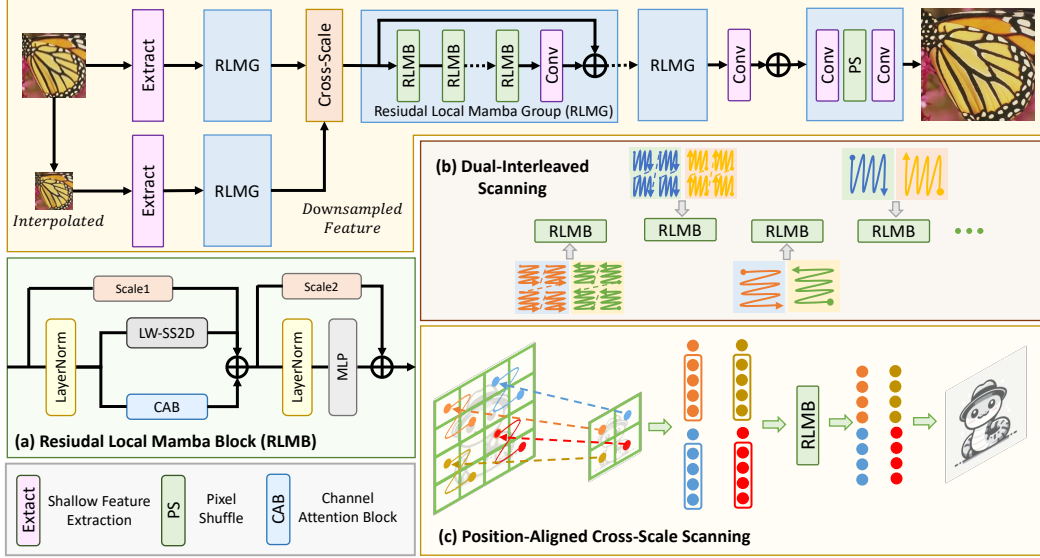


Figure 2: The Overall Architecture of MambaCSR. The overall pipeline (top) consists of three components: shallow feature extraction, deep feature extraction, and high-resolution reconstruction. (b) illustrates our proposed dual-interleaved scanning method. (c) represents the process of cross-scale scanning for fusing multi-scale features.

3.1 Preliminaries

Preliminary. State space model (SSM) is excellent at processing long linear sequences. Given a one-dimensional sequence input $x(t)$, SSM aims to output $y(t)$ through latent states $h(t)$ and input $x(t)$ as follows:

$$\begin{aligned} h'(t) &= Ah(t) + Bx(t), \\ y(t) &= Ch(t) + Dx(t). \end{aligned} \quad (1)$$

Here A, B, C, D are four preset model parameters. As a discrete variant of SSM, mamba utilizes zero-order hold (ZOH) to discretize the process above while allowing an adaptive selective scanning mechanism for input data. The discretized values of A and B could be denoted as \bar{A} and \bar{B} . Thus, Eq. 1 could be reformulated as follows:

$$\begin{aligned} \bar{A} &= e^{\Delta A}, \\ \bar{B} &= (\Delta A)^{-1}(e^{\Delta A} - I) \odot \Delta B, \\ h(t) &= \bar{A}h(t-1) + \bar{B}x(t), \\ y(t) &= Ch(t) + Dx(t). \end{aligned} \quad (2)$$

Finally, the output could be obtained through a global convolution as follows: (\bar{K} denotes the convolution kernel.)

$$y = x \odot \bar{K}, \quad \bar{K} = (\bar{C}\bar{B}, \bar{C}\bar{A}\bar{B}, \dots, \bar{C}\bar{A}^{L-1}\bar{B}). \quad (3)$$

3.2 Motivations

Since the recurrent state space of Mamba, the contextual modeling in Mamba will vary for different scanning trajectories. To illustrate this, we can calculate the contribution of the p -th token on the q -th token following MSVMamba [41]:

$$\begin{aligned} C_q \prod_{i=p}^q \bar{A}_i \bar{B}_p &= C_q \bar{A}_{(p \rightarrow q)} \bar{B}_p, \\ \bar{A}_{(p \rightarrow q)} &= e^{\sum_{i=p}^q \Delta_i \mathbf{A}}. \end{aligned} \quad (4)$$

The $\Delta_i \mathbf{A}$ in Eq. 4 is negative, indicating that as the number of scanned tokens increases, the contextual information of earlier scanned tokens on the current one is diminished. This also implies that the sequential scanning method shown in Fig. 1(a) may overlook some local dependencies between adjacent tokens. In contrast, window-based scanning [19] shown in Fig. 1(b) excel at modeling local contextual information by narrowing the distance between adjacent tokens in the scanning trajectory with widow partition.

A well-designed scanning strategy is crucial for the representation capability of the Mamba framework. In terms of CSR tasks, the degradations are usually diverse, severe, and non-uniformed, which poses high requirements for comprehensive contextual information excavation. To achieve this, we propose a hierarchical interleaved scanning approach that iteratively leverages the window-based and sequential scanning methods for joint excavation of local and long-range contextual information. Additionally, to eliminate the redundancy between four types of scanning directions for contextual modeling, we decouple it into interleaved horizontal and vertical scanning trajectories in adjacent layers, resulting in our horizontal-to-vertical scanning strategy. The above two scanning strategies contribute to our dual-interleaved scanning paradigm for CSR.

3.3 Dual-Interleaved Scanning (DIS).

As shown in Fig. 2(b), we employ a dual-interleaved scanning approach to enhance the modeling of local dependencies and long-range contextual information, while also improving computational efficiency. This approach interleaves two types of scanning: (i) Hierarchical interleaved scanning is applied every two blocks to balance local and global feature extraction. (ii) Interleaved horizontal-to-vertical scanning. The original scanning method includes four scans, which introduces computational redundancy; consequently, one scanning path might dominate the critical information, while the others contribute less (Shi, Dong, and Xu 2024). To address this, we reduce the four directional scans to two horizontal and two vertical scans, with each block undergoing only two scans. Crucially, we ensure that each scan is paired with its flipped counterpart. This pairing is necessary due to the non-causality of Mamba, where only preceding tokens contribute to subsequent tokens within a sequence. Paired scanning is therefore essential to ensure bidirectional information flow.

3.4 Position-Aligned Cross-Scale Scanning.

Compressed image super-resolution tasks necessitate the handling of non-uniform compression artifacts, which demand richer contextual information. In this paper, we propose a novel position-aligned cross-scale scanning method to deliver multi-scale contextual information, as illustrated in Fig. 2(c). Specifically, as illustrated on the top-left side of Fig. 2, the down-sampled image is generated through interpolation from the original image (scaling factor = 0.5), followed by shallow feature extraction and one RLMG layer. Each token in the down-sampled image corresponds to four tokens in the original image. Our core approach is to model four corresponding positions in the original feature map using each token in the down-sampled feature map. To clarify this process, we assume the down-sampled feature map is represented by the matrix:

$$\mathbf{X} = \begin{pmatrix} \mathbf{x}^{(0,0)} & \mathbf{x}^{(0,1)} & \dots & \mathbf{x}^{(0,\mathcal{W}-1)} \\ \mathbf{x}^{(1,0)} & \mathbf{x}^{(1,1)} & \dots & \mathbf{x}^{(1,\mathcal{W}-1)} \\ \vdots & \vdots & \ddots & \vdots \\ \mathbf{x}^{(\mathcal{H}-1,0)} & \mathbf{x}^{(\mathcal{H}-1,1)} & \dots & \mathbf{x}^{(\mathcal{H}-1,\mathcal{W}-1)} \end{pmatrix} \quad (5)$$

The original feature map could be represented by:

$$\mathbf{Y} = \begin{pmatrix} \mathbf{y}^{(0,0)} & \mathbf{y}^{(0,1)} & \dots & \mathbf{y}^{(0,2\mathcal{W}-1)} \\ \mathbf{y}^{(1,0)} & \mathbf{y}^{(1,1)} & \dots & \mathbf{y}^{(1,2\mathcal{W}-1)} \\ \vdots & \vdots & \ddots & \vdots \\ \mathbf{y}^{(2\mathcal{H}-1,0)} & \mathbf{y}^{(2\mathcal{H}-1,1)} & \dots & \mathbf{y}^{(2\mathcal{H}-1,2\mathcal{W}-1)} \end{pmatrix} \quad (6)$$

For each token $\mathbf{x}^{(i,j)}$ in the down-sampled feature, we sequentially scan the four corresponding positions in the original feature: $\mathbf{Y}^{(2i,2j)}$, $\mathbf{Y}^{(2i+1,2j)}$, $\mathbf{Y}^{(2i,2j+1)}$, and $\mathbf{Y}^{(2i+1,2j+1)}$ tokens. Then, we alternately scan the down-sampled features and the original features, unfold them into a 1D sequence, and feed this sequence into the RLMB for information interaction. This method ensures

that the downsampled tokens, which exist at a 1:4 ratio within the 1D sequence, contribute effectively to the modeling of tokens in the original feature map. After processing through the Mamba Block, the tokens corresponding to the downsampled features are removed, retaining only those associated with the original image. This selective scanning approach optimizes the fusion of multi-scale features. Importantly, to conserve parameters and reduce computational complexity, this fusion process is applied only after the first RLMG block.

3.5 Network Architecture

Followed by previous SR works [5, 28, 29], the overall architecture can be split into three components shown in the top of Fig. 2: shallow feature extraction, deep feature extraction, and high-resolution reconstruction. Given a input compressed low resolution image $I_{LR} \in \mathbb{R}^{H \times W \times C_{in}}$, where H , W , C_{in} denote the height, width, channel dimension of input I_{LR} . We first use a single convolution layer of kernel size 3×3 to extract shallow features of I_{LR} :

$$F_0 = f_{sfe}(I_{LR}) \quad (7)$$

Then, we use several Residual Local Mamba Groups (RLMG) and one convolution layer to further extract deep features of F_0 . The output deep features $F_1 \in \mathbb{R}^{H \times W \times C}$ can be expressed as:

$$F_1 = f_{conv}(f_{rlmg}^n \dots (f_{rlmg}^2 (f_{rlmg}^1 (F_0)))) + F_0 \quad (8)$$

We employ a residual connection to fuse the shallow feature F_0 with the deep feature F_1 . Each RLMG consists of several Residual Local Mamba Blocks (RLMB), detailed in Sec.3.5, along with a convolutional layer. Additionally, we generate a down-sampled image from the original using interpolation, process it through a convolutional layer and one RLMG, and then integrate it with the original image features via the position-aligned cross-scale module. Finally, for high-resolution reconstruction, we apply a pixel-shuffle layer to up-sample the fused feature. We optimize our MambaCSR following previous CSR works [23, 8] with L_1 Loss:

$$\mathcal{L} = \|I_{HR} - I_{LR}\|_1, \quad (9)$$

Residual Local Mamba Block (RLMB).

The Residual Local Mamba Block (RLMB) focuses on deep modeling of input features, capturing both local and long-range information. In each block, we first apply a normalization layer, followed by the adoption of a local-window-based 2D Selective Scan Module (LW-SS2D) to capture spatial long-range dependencies, as shown in Fig. 1 (b). We use different window sizes to represent local window-based and sequential scanning methods. For an input image size of 64×64 during the training phase, the window size for local scanning is set to 8, while the window size for sequential scanning is set to 64. Inspired by work HAT [5], we also employ channel attention block parallel to LW-SS2D to further enhance the representation ability of the network. Followed by MambaIR [15], we use a scaling factor s_1 to control the intensity of input feature X through skip connection. After establishing long-term relationships, we apply Layer normalization and MLP to process the intermediate features. Scaling factor s_2 is also used to control the magnitude of residual. Thus, the entire process of RLMB could be expressed as:

$$\begin{aligned} F_{inter} &= \text{CAB}(\text{LN}(X)) + \text{LW-SSM}(\text{LN}(X)) + s_1 X \\ F_{out} &= s_2 F_{inter} + \text{MLP}(\text{LN}(F_{inter})) \end{aligned} \quad (10)$$

Here, F_{inter} denotes the intermediate features.

4 Experiments

In this section, we first describe the dataset and implementation details in Sec. 4.1. Next, we compare our proposed MambaCSR with current state-of-the-art CSR methods and present the visual results in Sec. 4.2. Finally, to validate the effectiveness of our proposed dual-interleaved scanning and cross-scale scanning method, we conduct a series of ablation studies, as detailed in Sec. 4.3.

Methods	Cost		Datasets									
			Set5		Set14		Manga109		Urban100		DIV2K Test	
	Params (M)	GFLOPS	PSNR	SSIM	PSNR	SSIM	PSNR	SSIM	PSNR	SSIM	PSNR	SSIM
RCAN	15.59	65.25	24.87	0.7019	23.72	0.5983	22.65	0.7128	21.58	0.5795	24.77	0.6639
SwinIR	8.72	37.17	25.10	0.7152	23.97	0.6027	23.31	0.7354	22.03	0.6004	25.61	0.6861
Swin2SR	11.67	52.96	25.12	0.7162	23.96	0.6028	23.35	0.7358	22.08	0.6008	25.64	0.6868
HST	16.48	54.95	25.12	0.7156	24.00	0.6034	23.39	0.7365	22.10	0.6026	25.66	0.6887
HAT	20.81	102.4	25.13	0.7177	24.02	0.6052	23.42	0.7362	22.13	0.6037	25.66	0.6895
MambaIR	16.70	82.30	25.13	0.7176	24.01	0.6054	23.46	0.7379	22.14	0.6041	25.68	0.6894
MambaCSR (w/o)	16.91	75.01	25.16	0.7201	24.06	0.6065	23.52	0.7400	22.22	0.6071	25.72	0.6906
MambaCSR (Final)	19.18	80.46	25.20	0.7209	24.07	0.6072	23.57	0.7419	22.26	0.6081	25.74	0.6911

Table 1: Quantitative comparison for compressed image super-resolution on JPEG [46] codec with quality factor 10. The best performance is in **bold**. Results tested on different metrics in terms of PSNR \uparrow , SSIM \uparrow . We release two versions of MambaCSR, one is without (w/o) cross-scale scanning, and the other is with cross-scale scanning (Final).

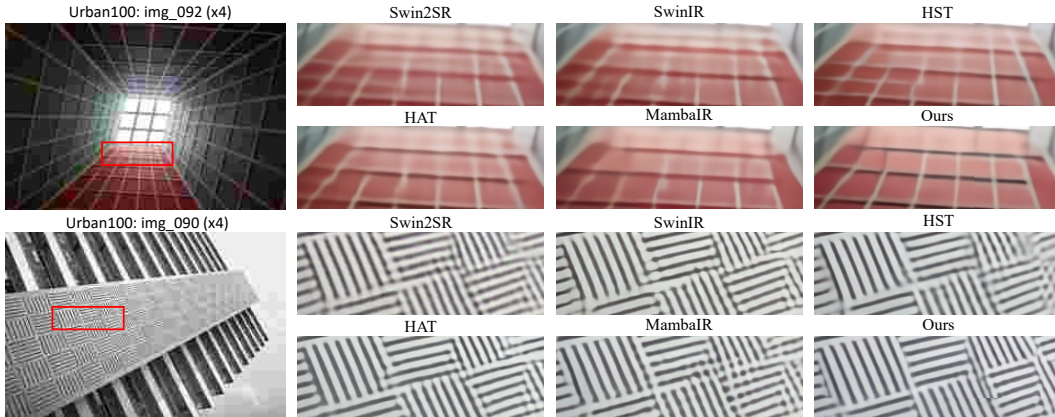


Figure 3: Visual comparison of our MambaCSR with other SOTA models on Urban100 with scale x4.

4.1 Dataset and Implementation Details

We use the DF2K [1] dataset as our primary training dataset. Given that JPEG [46] is currently the most widely used compression standard, we apply JPEG compression with quality factors from range [10, 20, 30] to the dataset using the JPEG codec function provided by the OpenCV library. For evaluation, we test on five commonly used super-resolution benchmarks: Set5 [2], Set14 [63], Manga109 [34], Urban100 [18], and the DIV2K test set [1]. The entire implementation is based on the PyTorch framework. During training, we employ the Adam optimizer ($\beta_1=0.9$, $\beta_2=0.99$) with an initial learning rate of $2e-4$, which is decayed by a factor of 0.5 at 150k, 225k, and 275k iterations. Due to the small size of the DF2K dataset and its rapid convergence, the total number of iterations is set to 300k. Input low-resolution images are randomly cropped to 64×64 and augmented with random flips and rotations. The window size for interleaved scanning is set to 8. The total batch size is set to 32, trained on eight NVIDIA V100 GPUs.

4.2 Comparison with State-of-the-Art

We compare our proposed MambaCSR with three image super-resolution models: RCAN [68], SwinIR [28], and HAT [5]. Additionally, we include two state-of-the-art compressed image super-resolution models: Swin2SR [8] and HST [23], as well as the SSM-based baseline model, MambaIR [15]. All models are trained on the compressed DF2K dataset using the same settings. For evaluation, we employ PSNR and SSIM metrics, with PSNR values specifically measured on the Y channel.

Quantitative Results. From Table 1, it is evident that our proposed MambaCSR achieves the best performance across all five compressed benchmarks in terms of PSNR and SSIM. Specifically, on the Manga109 and Urban100 datasets, MambaCSR with cross-scale scanning outperforms MambaIR by an average of 0.12 dB, highlighting the effectiveness of our framework. We attribute this

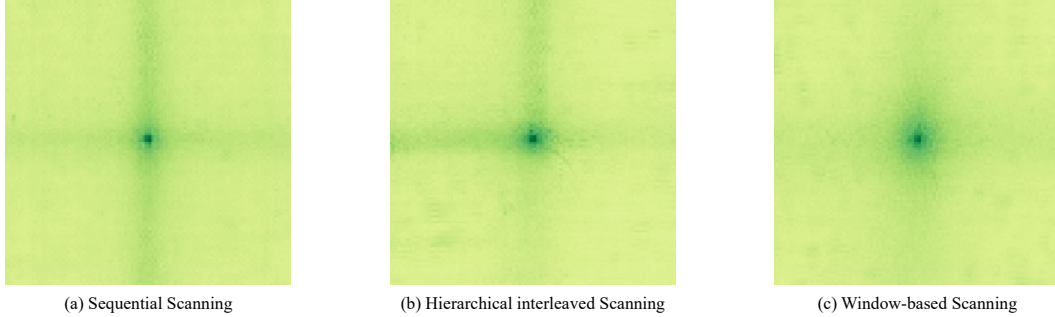


Figure 4: The receptive fields of different scanning methods: (a) Sequential scanning adopted in MambaIR, (b) Our hierarchical interleaved scanning, (c) Only local window-based scanning. All results are tested on the Manga109 dataset.

Window Size	Manga109		Urban100	
	PSNR	SSIM	PSNR	SSIM
4×4	23.49	0.7394	22.19	0.6059
8×8	23.53	0.7400	22.22	0.6071
16×16	23.51	0.7396	22.20	0.6065
32×32	23.47	0.7377	22.17	0.6043
64×64	23.47	0.7374	22.14	0.6036

Table 2: The effect of window size used in dual-interleaved scanning. The best performance is in methods: (I) our position-aligned cross-scale scanning. (II) simple sequential scanning.

Scanning Methods	Manga109		Urban100	
	PSNR	SSIM	PSNR	SSIM
No scanning	23.53	0.7400	22.22	0.6071
Position-Aligned	23.57	0.7419	22.26	0.6081
Sequential Scanning	23.53	0.7403	22.24	0.6077

improvement to the introduction of dual-interleaved scanning, which enhances the model’s focus on local information, and the use of cross-scale scanning, which better leverages multi-scale features for removing compression and downsampled artifacts. Additional results under different quality factor settings [20, 30] are provided in the Sec. A.3 of **supplementary**.

Qualitative Results. We present visual comparisons with other models. As shown in Fig. 3, our proposed MambaCSR excels in handling compression artifacts, particularly in restoring textures and fine details, highlighting the robustness of our model.

Computational Comparisons. To demonstrate the efficiency of our dual-interleaved scanning method, we evaluate the parameter count and computational complexity of the proposed modules and compare them with other models. As shown in Table 1, the computational cost of using only the dual-interleaved scanning method is 10 GFLOPS lower than that of MambaIR. Even when incorporating cross-scale scanning, our computational complexity remains comparable to MambaIR, highlighting the efficiency of the dual-interleaved scanning method.

4.3 Ablation Studies

Effects of window-size used in dual-interleaved scanning. We introduce an interleaved hierarchical scanning approach to capture both local and global information from compressed images. In window-based local scanning, images are divided into regions according to the window size. To determine the optimal window size, we conduct ablation studies without cross-scale scanning. Given that the input low-resolution images during training are 64×64 , we test five window sizes: 64×64 , 32×32 , 16×16 , 8×8 , and 4×4 , and tested the results on Manga109 and Urban100 datasets. As shown in Table 2, the 8×8 window size strikes the best balance for effectively capturing local information.

Effects of different cross-scale scanning methods. In this paper, we introduce the position-aligned cross-scale scanning method, as shown in Fig. 2(c). To validate the effectiveness of our position-aligned approach, we also implement a sequential scanning method, where all tokens of the low-resolution image are scanned first, followed by scanning the tokens of the high-resolution image. We then compare the performance of these two approaches. As shown in Table 3, the position-aligned cross-scale scanning method outperforms the sequential scanning approach. This indicates that the

position-aligned method is more effective in modeling multi-scale features. The likely reason for the underperformance of the simple sequential scanning approach is that the long-sequence decay properties inherent to the SSM reduce the influence of low-resolution tokens on the original feature tokens.

Effects of dual-interleaved scanning and CAB. To validate the effectiveness of our proposed dual-interleaved scanning method and the channel attention block used in each RLMB, we separately test the hierarchical interleaved scanning and horizontal-to-vertical interleaved scanning components within the dual-interleaved framework. As shown in Table 4, hierarchical interleaved scanning yields the highest performance gain, followed by the channel attention block. Although the performance of horizontal-to-vertical scanning alone shows a slight decrease, its integration with the other two methods maintains comparable performance while offering the advantage of reduced computational complexity. This demonstrates the capability of the dual-interleaved scanning method to balance performance gains with reduced computational complexity. We also present the receptive fields of different scanning methods, including sequential scanning, window-based scanning, and our proposed hierarchical-interleaved scanning. As depicted in Fig. 4, the sequential scanning method exhibits a smaller central receptive field while maintaining some level of global information perception. In contrast, window-based scanning enhances the local receptive field in the center but loses some capacity for global information modeling. Our hierarchical interleaved scanning method, on the other hand, balances local and global receptive fields, retaining the long-range modeling capacity while providing a larger local receptive field compared to the sequential scanning method.

Hierarchical	Horizontal-to-vertical	CAB	Manga109	Urban100
X	X	X	23.44	22.12
✓	X	X	23.49	22.18
X	✓	X	23.43	22.11
X	X	✓	23.47	22.15
✓	✓	X	23.48	22.16
✓	X	✓	23.53	22.22
X	✓	✓	23.47	22.14
✓	✓	✓	23.52	22.20

Table 4: Effects of hierarchical interleaved scanning, horizontal-to-vertical interleaved scanning and CAB. The performance is tested on Manga109. The best performance is in **bold**.

5 Conclusion

In this paper, we introduce MambaCSR, the first Mamba-based framework for compressed image super-resolution. Concretely, we investigate the effects of different scanning strategies for the contextual modeling of CSR, and propose the efficient dual-interleaved scanning (DIS) paradigm for CSR, intending to activate comprehensive contextual modeling of Mamba. The DIS is composed of hierarchical interleaved scanning, which aims to excavate the local and long-range contextual information simultaneously, and horizontal-to-vertical interleaved scanning to reduce the computational redundancy caused by four types of scanning trajectories in Mamba. To overcome the non-uniformed compression degradation and further enhance CSR performance, we develop a novel position-aligned cross-scale scanning method that effectively fuses multi-scale features. The experimental results across various compressed benchmarks demonstrate the advantages of our dual-interleaved scanning approach and validate the superiority of the position-aligned cross-scale scanning method. We also analyze the limitations and broad impacts of our MambaCSR in the **supplementary**.

References

- [1] E. Agustsson and R. Timofte. Ntire 2017 challenge on single image super-resolution: Dataset and study. In *The IEEE Conference on Computer Vision and Pattern Recognition (CVPR) Workshops*, July 2017.

- [2] M. Bevilacqua, A. Roumy, C. Guillemot, and M. L. Alberi-Morel. Low-complexity single-image super-resolution based on nonnegative neighbor embedding. 2012.
- [3] B. Bross, Y.-K. Wang, Y. Ye, S. Liu, J. Chen, G. J. Sullivan, and J.-R. Ohm. Overview of the versatile video coding (vvc) standard and its applications. *IEEE Transactions on Circuits and Systems for Video Technology*, 31(10):3736–3764, 2021.
- [4] H. Chen, Y. Wang, T. Guo, C. Xu, Y. Deng, Z. Liu, S. Ma, C. Xu, C. Xu, and W. Gao. Pre-trained image processing transformer. In *Proceedings of the IEEE/CVF conference on computer vision and pattern recognition*, pages 12299–12310, 2021.
- [5] X. Chen, X. Wang, J. Zhou, Y. Qiao, and C. Dong. Activating more pixels in image super-resolution transformer. In *Proceedings of the IEEE/CVF conference on computer vision and pattern recognition*, pages 22367–22377, 2023.
- [6] Z. Chen, Z. Wu, E. Zamfir, K. Zhang, Y. Zhang, R. Timofte, X. Yang, H. Yu, C. Wan, Y. Hong, et al. Ntire 2024 challenge on image super-resolution (x4): Methods and results. In *Proceedings of the IEEE/CVF Conference on Computer Vision and Pattern Recognition*, pages 6108–6132, 2024.
- [7] C. Cheng, H. Wang, and H. Sun. Activating wider areas in image super-resolution. *arXiv preprint arXiv:2403.08330*, 2024.
- [8] M. V. Conde, U.-J. Choi, M. Burchi, and R. Timofte. Swin2sr: Swinv2 transformer for compressed image super-resolution and restoration. In *European Conference on Computer Vision*, pages 669–687. Springer, 2022.
- [9] T. Dai, J. Cai, Y. Zhang, S.-T. Xia, and L. Zhang. Second-order attention network for single image super-resolution. In *Proceedings of the IEEE/CVF conference on computer vision and pattern recognition*, pages 11065–11074, 2019.
- [10] C. Dong, C. C. Loy, K. He, and X. Tang. Image super-resolution using deep convolutional networks. *IEEE transactions on pattern analysis and machine intelligence*, 38(2):295–307, 2015.
- [11] C. Dong, C. C. Loy, and X. Tang. Accelerating the super-resolution convolutional neural network. In *Computer Vision—ECCV 2016: 14th European Conference, Amsterdam, The Netherlands, October 11–14, 2016, Proceedings, Part II 14*, pages 391–407. Springer, 2016.
- [12] A. Gu and T. Dao. Mamba: Linear-time sequence modeling with selective state spaces. *arXiv preprint arXiv:2312.00752*, 2023.
- [13] A. Gu, K. Goel, and C. Ré. Efficiently modeling long sequences with structured state spaces. *arXiv preprint arXiv:2111.00396*, 2021.
- [14] F. Guan, X. Li, Z. Yu, Y. Lu, and Z. Chen. Q-mamba: On first exploration of vision mamba for image quality assessment. *arXiv preprint arXiv:2406.09546*, 2024.
- [15] H. Guo, J. Li, T. Dai, Z. Ouyang, X. Ren, and S.-T. Xia. Mambair: A simple baseline for image restoration with state-space model. *arXiv preprint arXiv:2402.15648*, 2024.
- [16] X. He, K. Cao, K. Yan, R. Li, C. Xie, J. Zhang, and M. Zhou. Pan-mamba: Effective pan-sharpening with state space model. *arXiv preprint arXiv:2402.12192*, 2024.
- [17] Y. Hu, W. Yang, and J. Liu. Coarse-to-fine hyper-prior modeling for learned image compression. In *Proceedings of the AAAI Conference on Artificial Intelligence*, volume 34, pages 11013–11020, 2020.
- [18] J.-B. Huang, A. Singh, and N. Ahuja. Single image super-resolution from transformed self-exemplars. In *Proceedings of the IEEE conference on computer vision and pattern recognition*, pages 5197–5206, 2015.
- [19] T. Huang, X. Pei, S. You, F. Wang, C. Qian, and C. Xu. Localmamba: Visual state space model with windowed selective scan. *arXiv preprint arXiv:2403.09338*, 2024.

- [20] J. Kim, J. K. Lee, and K. M. Lee. Accurate image super-resolution using very deep convolutional networks. In *Proceedings of the IEEE conference on computer vision and pattern recognition*, pages 1646–1654, 2016.
- [21] X. Lei, W. ZHANG, and W. Cao. Dvmsr: Distillated vision mamba for efficient super-resolution. *arXiv preprint arXiv:2405.03008*, 2024.
- [22] B. Li, X. Li, Y. Lu, R. Feng, M. Guo, S. Zhao, L. Zhang, and Z. Chen. Promptcir: Blind compressed image restoration with prompt learning. *arXiv preprint arXiv:2404.17433*, 2024.
- [23] B. Li, X. Li, Y. Lu, S. Liu, R. Feng, and Z. Chen. Hst: Hierarchical swin transformer for compressed image super-resolution. In *European conference on computer vision*, pages 651–668. Springer, 2022.
- [24] X. Li, X. Jin, T. Yu, S. Sun, Y. Pang, Z. Zhang, and Z. Chen. Learning omni-frequency region-adaptive representations for real image super-resolution. In *Proceedings of the AAAI Conference on Artificial Intelligence*, volume 35, pages 1975–1983, 2021.
- [25] X. Li, B. Li, Y. Jin, C. Lan, H. Zhu, Y. Ren, and Z. Chen. Ucip: A universal framework for compressed image super-resolution using dynamic prompt. *arXiv preprint arXiv:2407.13108*, 2024.
- [26] X. Li, J. Shi, and Z. Chen. Task-driven semantic coding via reinforcement learning. *IEEE Transactions on Image Processing*, 30:6307–6320, 2021.
- [27] D. Liang, X. Zhou, X. Wang, X. Zhu, W. Xu, Z. Zou, X. Ye, and X. Bai. Pointmamba: A simple state space model for point cloud analysis. *arXiv preprint arXiv:2402.10739*, 2024.
- [28] J. Liang, J. Cao, G. Sun, K. Zhang, L. Van Gool, and R. Timofte. Swinir: Image restoration using swin transformer. In *Proceedings of the IEEE/CVF international conference on computer vision*, pages 1833–1844, 2021.
- [29] B. Lim, S. Son, H. Kim, S. Nah, and K. Mu Lee. Enhanced deep residual networks for single image super-resolution. In *Proceedings of the IEEE conference on computer vision and pattern recognition workshops*, pages 136–144, 2017.
- [30] Y. Liu, Y. Tian, Y. Zhao, H. Yu, L. Xie, Y. Wang, Q. Ye, and Y. Liu. Vmamba: Visual state space model. *arXiv preprint arXiv:2401.10166*, 2024.
- [31] Y. Lu, S. Wang, Z. Wang, P. Xia, T. Zhou, et al. Lfmamba: Light field image super-resolution with state space model. *arXiv preprint arXiv:2406.12463*, 2024.
- [32] Z. Lu, J. Li, H. Liu, C. Huang, L. Zhang, and T. Zeng. Transformer for single image super-resolution. In *Proceedings of the IEEE/CVF conference on computer vision and pattern recognition*, pages 457–466, 2022.
- [33] J. Ma, F. Li, and B. Wang. U-mamba: Enhancing long-range dependency for biomedical image segmentation. *arXiv preprint arXiv:2401.04722*, 2024.
- [34] Y. Matsui, K. Ito, Y. Aramaki, A. Fujimoto, T. Ogawa, T. Yamasaki, and K. Aizawa. Sketch-based manga retrieval using manga109 dataset. *Multimedia tools and applications*, 76:21811–21838, 2017.
- [35] Y. Mei, Y. Fan, and Y. Zhou. Image super-resolution with non-local sparse attention. In *Proceedings of the IEEE/CVF conference on computer vision and pattern recognition*, pages 3517–3526, 2021.
- [36] F. Mentzer, G. D. Toderici, M. Tschannen, and E. Agustsson. High-fidelity generative image compression. *Advances in Neural Information Processing Systems*, 33:11913–11924, 2020.
- [37] H. Qin, Y. Zhang, Y. Ding, X. Liu, M. Danelljan, F. Yu, et al. Quantsr: accurate low-bit quantization for efficient image super-resolution. *Advances in Neural Information Processing Systems*, 36, 2024.

- [38] X. Qin, Y. Zhu, C. Li, P. Wang, and J. Cheng. Cidbnet: a consecutively-interactive dual-branch network for jpeg compressed image super-resolution. In *European Conference on Computer Vision*, pages 458–474. Springer, 2022.
- [39] Y. Ren, X. Li, B. Li, X. Wang, M. Guo, S. Zhao, L. Zhang, and Z. Chen. Moe-diffir: Task-customized diffusion priors for universal compressed image restoration. *arXiv preprint arXiv:2407.10833*, 2024.
- [40] Q. Shen, X. Yi, Z. Wu, P. Zhou, H. Zhang, S. Yan, and X. Wang. Gamba: Marry gaussian splatting with mamba for single view 3d reconstruction. *arXiv preprint arXiv:2403.18795*, 2024.
- [41] Y. Shi, M. Dong, and C. Xu. Multi-scale vmamba: Hierarchy in hierarchy visual state space model. *arXiv preprint arXiv:2405.14174*, 2024.
- [42] Y. Shi, B. Xia, X. Jin, X. Wang, T. Zhao, X. Xia, X. Xiao, and W. Yang. Vmambair: Visual state space model for image restoration. *arXiv preprint arXiv:2403.11423*, 2024.
- [43] V. Sze, M. Budagavi, and G. J. Sullivan. High efficiency video coding (hevc). In *Integrated circuit and systems, algorithms and architectures*, volume 39, page 40. Springer, 2014.
- [44] Y. Teng, Y. Wu, H. Shi, X. Ning, G. Dai, Y. Wang, Z. Li, and X. Liu. Dim: Diffusion mamba for efficient high-resolution image synthesis. *arXiv preprint arXiv:2405.14224*, 2024.
- [45] R. Timofte, E. Agustsson, L. Van Gool, M.-H. Yang, and L. Zhang. Ntire 2017 challenge on single image super-resolution: Methods and results. In *Proceedings of the IEEE conference on computer vision and pattern recognition workshops*, pages 114–125, 2017.
- [46] G. K. Wallace. The jpeg still picture compression standard. *Communications of the ACM*, 34(4):30–44, 1991.
- [47] Z. Wan, Y. Wang, S. Yong, P. Zhang, S. Stepputtis, K. Sycara, and Y. Xie. Sigma: Siamese mamba network for multi-modal semantic segmentation. *arXiv preprint arXiv:2404.04256*, 2024.
- [48] J. Wang, Z. Yue, S. Zhou, K. C. Chan, and C. C. Loy. Exploiting diffusion prior for real-world image super-resolution. *International Journal of Computer Vision*, pages 1–21, 2024.
- [49] P. Wei, H. Lu, R. Timofte, L. Lin, W. Zuo, Z. Pan, B. Li, T. Xi, Y. Fan, G. Zhang, et al. Aim 2020 challenge on real image super-resolution: Methods and results. In *Computer Vision–ECCV 2020 Workshops: Glasgow, UK, August 23–28, 2020, Proceedings, Part III 16*, pages 392–422. Springer, 2020.
- [50] H. Wu, Y. Yang, H. Xu, W. Wang, J. Zhou, and L. Zhu. Rainmamba: Enhanced locality learning with state space models for video deraining. *arXiv preprint arXiv:2407.21773*, 2024.
- [51] R. Wu, T. Yang, L. Sun, Z. Zhang, S. Li, and L. Zhang. Seesr: Towards semantics-aware real-world image super-resolution. In *Proceedings of the IEEE/CVF conference on computer vision and pattern recognition*, pages 25456–25467, 2024.
- [52] Y. Wu, X. Li, Z. Zhang, X. Jin, and Z. Chen. Learned block-based hybrid image compression. *IEEE Transactions on Circuits and Systems for Video Technology*, 32(6):3978–3990, 2021.
- [53] B. Xia, Y. Hang, Y. Tian, W. Yang, Q. Liao, and J. Zhou. Efficient non-local contrastive attention for image super-resolution. In *Proceedings of the AAAI conference on artificial intelligence*, volume 36, pages 2759–2767, 2022.
- [54] J. Xie, R. Liao, Z. Zhang, S. Yi, Y. Zhu, and G. Luo. Promamba: Prompt-mamba for polyp segmentation. *arXiv preprint arXiv:2403.13660*, 2024.
- [55] Z. Xu, Y. Lin, H. Han, S. Yang, R. Li, Y. Zhang, and X. Li. Mambatalk: Efficient holistic gesture synthesis with selective state space models. *arXiv preprint arXiv:2403.09471*, 2024.

- [56] R. Yang, R. Timofte, B. Li, X. Li, M. Guo, S. Zhao, L. Zhang, Z. Chen, D. Zhang, Y. Arora, et al. Ntire 2024 challenge on blind enhancement of compressed image: Methods and results. In *Proceedings of the IEEE/CVF Conference on Computer Vision and Pattern Recognition*, pages 6524–6535, 2024.
- [57] R. Yang, R. Timofte, X. Li, Q. Zhang, L. Zhang, F. Liu, D. He, F. Li, H. Zheng, W. Yuan, et al. Aim 2022 challenge on super-resolution of compressed image and video: Dataset, methods and results. In *European Conference on Computer Vision*, pages 174–202. Springer, 2022.
- [58] Y. Yang, C. Ma, J. Yao, Z. Zhong, Y. Zhang, and Y. Wang. Remember: Referring image segmentation with mamba twister. *arXiv preprint arXiv:2403.17839*, 2024.
- [59] J. Yao, D. Hong, C. Li, and J. Chanussot. Spectralmamba: Efficient mamba for hyperspectral image classification. *arXiv preprint arXiv:2404.08489*, 2024.
- [60] J. Yoo, T. Kim, S. Lee, S. H. Kim, H. Lee, and T. H. Kim. Enriched cnn-transformer feature aggregation networks for super-resolution. In *Proceedings of the IEEE/CVF winter conference on applications of computer vision*, pages 4956–4965, 2023.
- [61] L. Yu, X. Li, Y. Li, T. Jiang, Q. Wu, H. Fan, and S. Liu. Dipnet: Efficiency distillation and iterative pruning for image super-resolution. In *Proceedings of the IEEE/CVF Conference on Computer Vision and Pattern Recognition*, pages 1692–1701, 2023.
- [62] Z. Yue, J. Wang, and C. C. Loy. Resshift: Efficient diffusion model for image super-resolution by residual shifting. *Advances in Neural Information Processing Systems*, 36, 2024.
- [63] R. Zeyde, M. Elad, and M. Protter. On single image scale-up using sparse-representations. In *Curves and Surfaces: 7th International Conference, Avignon, France, June 24-30, 2010, Revised Selected Papers 7*, pages 711–730. Springer, 2012.
- [64] J. Zhang, Y. Zhang, J. Gu, Y. Zhang, L. Kong, and X. Yuan. Accurate image restoration with attention retractable transformer. *arXiv preprint arXiv:2210.01427*, 2022.
- [65] K. Zhang, W. Zuo, S. Gu, and L. Zhang. Learning deep cnn denoiser prior for image restoration. In *Proceedings of the IEEE conference on computer vision and pattern recognition*, pages 3929–3938, 2017.
- [66] K. Zhang, W. Zuo, and L. Zhang. Learning a single convolutional super-resolution network for multiple degradations. In *Proceedings of the IEEE conference on computer vision and pattern recognition*, pages 3262–3271, 2018.
- [67] T. Zhang, X. Li, H. Yuan, S. Ji, and S. Yan. Point could mamba: Point cloud learning via state space model. *arXiv preprint arXiv:2403.00762*, 2024.
- [68] Y. Zhang, K. Li, K. Li, L. Wang, B. Zhong, and Y. Fu. Image super-resolution using very deep residual channel attention networks. In *Proceedings of the European conference on computer vision (ECCV)*, pages 286–301, 2018.
- [69] Y. Zhang, Y. Tian, Y. Kong, B. Zhong, and Y. Fu. Residual dense network for image super-resolution. In *Proceedings of the IEEE conference on computer vision and pattern recognition*, pages 2472–2481, 2018.
- [70] Z. Zhen, Y. Hu, and Z. Feng. Freqmamba: Viewing mamba from a frequency perspective for image deraining. *arXiv preprint arXiv:2404.09476*, 2024.
- [71] Z. Zheng and C. Wu. U-shaped vision mamba for single image dehazing. *arXiv preprint arXiv:2402.04139*, 2024.
- [72] Q. Zhu, P. Li, and Q. Li. Attention retractable frequency fusion transformer for image super resolution. In *Proceedings of the IEEE/CVF Conference on Computer Vision and Pattern Recognition*, pages 1756–1763, 2023.
- [73] W. Zou, H. Gao, W. Yang, and T. Liu. Wave-mamba: Wavelet state space model for ultra-high-definition low-light image enhancement. *arXiv preprint arXiv:2408.01276*, 2024.

A Supplementary Material

In this document, we first describe the broader impact and limitations of our paper in Sec. A.1 and Sec. A.2 respectively. After that, we provide more quantitative results in Sec. A.3. Finally, we show more visual comparisons in Sec. A.4.

A.1 Broader Impact

MambaCSR, as proposed in this paper, introduces an innovative dual-interleaved scanning paradigm for compressed image super-resolution (CSR). By leveraging hierarchical interleaved scanning and horizontal-to-vertical scanning, MambaCSR significantly reduces redundancy while enhancing contextual information modeling, leading to more efficient and accurate super-resolution. These advancements not only improve the performance of CSR tasks in industrial applications but also contribute to reducing the computational burden associated with processing high-resolution images. The primary applications of MambaCSR span a range of areas, including image restoration, multimedia content enhancement, and visual communication. Importantly, the deployment of MambaCSR adheres to ethical standards, ensuring that the technology is used responsibly to avoid potential biases and harms in visual data processing. By focusing on efficiency and accuracy, MambaCSR paves the way for more sustainable and equitable advancements in the field of image processing.

A.2 Limitations

In this work, we introduce MambaCSR and propose dual-interleaved, position-aligned cross-scale scanning methods. While our approach demonstrates state-of-the-art performance on JPEG-compressed image super-resolution tasks, the generalization of MambaCSR to other compression standards remains unexplored. The CSR field encompasses a wide range of compression methods beyond JPEG, including traditional codecs such as VVC [3] and HEVC [43, 26], as well as newer, learning-based codecs [52, 17] like HIFIC [36]. The applicability of MambaCSR across these diverse compression techniques is still an open question. Future work will aim to evaluate MambaCSR’s performance on various compression standards and explore universal restoration methods. Additionally, the current training speed of MambaCSR for low-level tasks is relatively slow. Addressing this limitation will involve investigating more efficient training strategies and network designs to enhance MambaCSR’s training efficiency in future research.

Methods	Cost		Datasets									
			Set5		Set14		Manga109		Urban100		DIV2K Test	
	Params	FLops	PSNR	SSIM	PSNR	SSIM	PSNR	SSIM	PSNR	SSIM	PSNR	SSIM
SwinIR	8.72	37.17	26.51	0.7622	25.03	0.6393	24.89	0.7809	23.04	0.6462	26.72	0.7182
Swin2SR	11.67	52.96	26.56	0.7631	25.05	0.6394	24.92	0.7810	23.07	0.6471	26.73	0.7187
HST	16.48	54.95	26.53	0.7625	25.02	0.6395	24.91	0.7808	23.06	0.6467	26.73	0.7184
HAT	20.81	102.4	26.57	0.7624	25.04	0.6397	24.93	0.7809	23.12	0.6491	26.74	0.7196
MambaIR	16.70	82.30	26.61	0.7640	25.11	0.6400	25.01	0.7830	23.13	0.6530	26.76	0.7201
MambaCSR	19.18	80.46	26.67	0.7680	25.13	0.6420	25.12	0.7880	23.24	0.6580	26.79	0.7204

Table 5: Quantitative comparison for compressed image super-resolution on JPEG [46] codec with quality factor 20. The best performance is in **bold**. Results tested on different metrics in terms of PSNR \uparrow , SSIM \uparrow .

Methods	Cost		Datasets									
			Set5		Set14		Manga109		Urban100		DIV2K Test	
	Params	FLops	PSNR	SSIM	PSNR	SSIM	PSNR	SSIM	PSNR	SSIM	PSNR	SSIM
SwinIR	8.72	37.17	27.48	0.7849	25.61	0.6596	25.79	0.8054	23.59	0.6725	27.28	0.7355
Swin2SR	11.67	52.96	27.51	0.7846	25.61	0.6594	25.81	0.8057	23.63	0.6731	27.30	0.7359
HST	16.48	54.95	27.49	0.7851	25.60	0.6595	25.8	0.8058	23.61	0.6765	27.31	0.7361
HAT	20.81	102.4	27.53	0.7856	25.61	0.6608	25.84	0.8077	23.67	0.6778	27.32	0.7369
MambaIR	16.70	82.30	27.56	0.7860	25.64	0.6600	25.87	0.8080	23.72	0.7900	27.34	0.7375
MambaCSR	19.18	80.46	27.63	0.7880	25.70	0.6630	26.01	0.8120	23.82	0.6825	27.39	0.7398

Table 6: Quantitative comparison for compressed image super-resolution on JPEG codec with quality factor 30. The best performance is in **bold**. Results tested on different metrics in terms of PSNR \uparrow , SSIM \uparrow .

A.3 More Quantitative Results

In this section, we present additional quantitative results that extend beyond the main text, specifically focusing on settings with quality factors of 20 and 30. We compare our approach against four transformer-based models: SwinIR [28], Swin2SR [8], HST [23], HAT [5], as well as one Mamba-based model, MambaIR [15]. The evaluation is conducted on five compressed benchmarks: Set5 [2], Set14 [63], Manga109 [34], Urban100 [18], and the DIV2K test set [1]. All benchmarks are compressed using OpenCV library functions. As shown in Table 5 and Table 6, our model achieves optimal performance across all benchmarks, notably outperforming MambaIR by an average of approximately 0.11-0.12dB on the Manga109 and Urban100 datasets. Furthermore, our computational complexity remains comparable to that of MambaIR, which further demonstrates the efficiency and effectiveness of our approach.

A.4 More Visual Results

In this section, we present additional visual comparisons for QF=20 and QF=30, as illustrated in Fig.5. From the first image with a quality factor of 20, it is clear that our MambaCSR model excels at removing compression artifacts, providing a more orderly restoration of textures and structural details compared to other models. At a quality factor of 30, our model demonstrates its ability to recover finer-grained textures. In contrast, while MambaIR produces smoother overall images, it lacks detailed local structural information, underscoring its limitations in capturing localized features. We attribute these improvements to our proposed hierarchical-interleaved scanning and position-aligned cross-scale scanning methods, which offer superior contextual information modeling relative to other models.

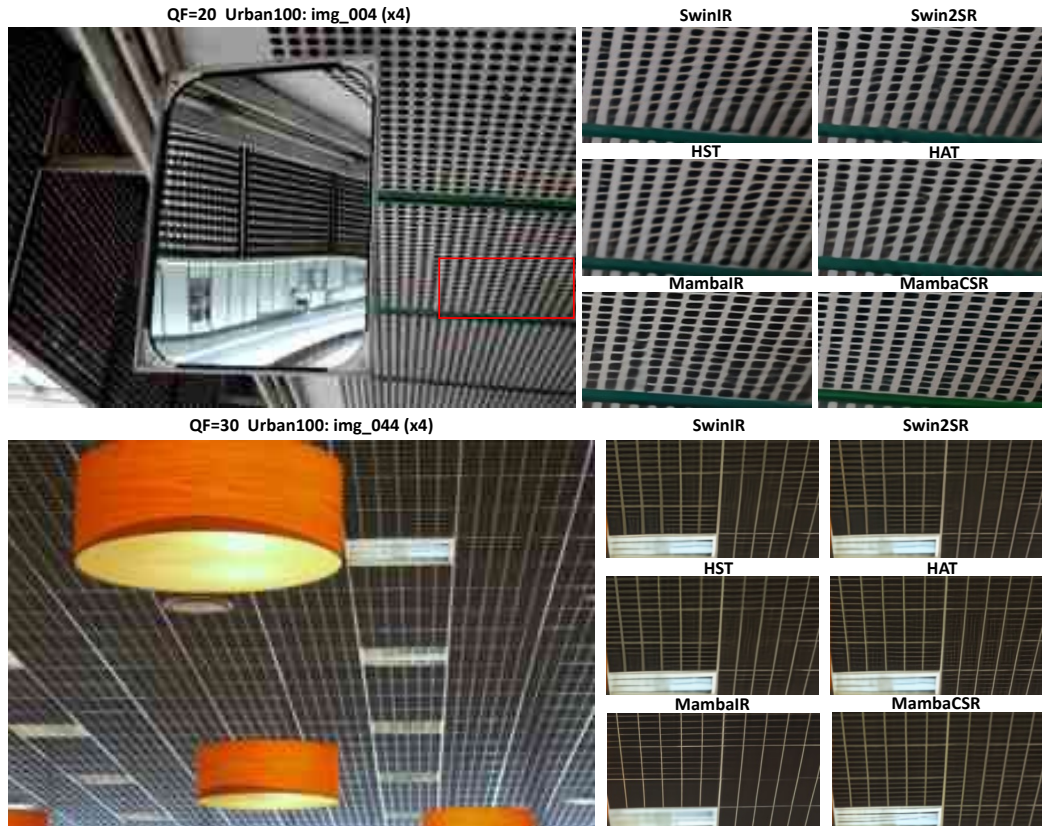


Figure 5: Visual Comparisons tested on Urban100 [18] at x4 scale of QF=[20,30].